

Hysteresis and creep in powders and grains

C. T. David, R. García-Rojo, H. J. Herrmann

Institute of Computer Physics, University of Stuttgart, Pfaffenwaldring, 27, 70569 Stuttgart, Germany

S. Luding

Particle Technology, DelftChemTech, TUDelft, Julianalaan 136, 2628 BL Delft, The Netherlands

ABSTRACT: The quasi-static mechanical response of grains under cyclic loading is studied in this contribution by means of a three-dimensional Molecular Dynamics scheme. The response of the system is characterized by an accumulation of plastic deformation with the number of cycles. For the deviatoric stress and strain, a quasi-periodic ratchet-like behavior is observed. Results are presented for different system sizes and coefficients of friction, respectively showing consistent results for more than ~ 2000 particles and much weaker plastic strain accumulation in the presence of stronger friction.

1 INTRODUCTION

The plastic behavior of a certain powder or soil sample depends on the history of the material (Vanel et al., 2004). Hysteretic behavior under repeated, cyclic loading is in fact a very relevant characteristic of granular materials. The extensive use of non-cohesive, dry granular materials in foundations of buildings and also as roadbeds, gives a clear idea of the urge for developing more efficient methods to study and understand the effects caused by cyclic loading.

Elementary tests are a straightforward way to determine empirical laws related to the behavior of powders and grains. They also permit the calculation of relevant parameters in constitutive laws. One possibility to perform these experiments is the triaxial setup, where the system is subjected to cyclic loading. Such tests are usually carried out in order to investigate the elasto-plastic response of granular materials. An alternative is the simulation of the system using discrete elements methods (DEM). In DEM the evolution of individual grains is obtained by the calculation of the interaction forces between particles. This includes, e.g., plastic deformations, cohesion and Coulomb friction. In the simplest case visco-elastic rules can be imposed at each contact, different for the normal and the tangential direction (Luding, 2004b). The system evolution is then obtained by integration of the equations of motion (Allen and Tildesley 1987).

All natural materials, when subject to continuous load, producing relatively high stress, exhibit defor-

mation and creep. Given a cyclic perturbation of a granular material, the main question is whether the material accumulates plastic deformation in each cycle or whether it adapts to the excitation. Only materials in which the excitations shake down, i.e. do not accumulate, should be consequently used.

The concept of ratcheting was introduced in soil mechanics in order to describe the gradual accumulation of a small permanent deformation (Lekarp et al., 2004). Ratcheting is however a much general concept that has also been studied, driven by the need of understanding steel behavior (Colak, 2003) or biophysical systems such as molecular motors (Astumian, 2003). In a 2D granular packing of discs, subjected to stress controlled cyclic loading, strain accumulations were identified as shakedown, or ratcheting, depending on the amplitude of the stress variations. This particular phenomenon has been intensively investigated in 2D (Alonso-Marroquin et al., 2004; Garcia-Rojo et al., 2004); first 3D results on cyclic loading are presented here.

2 MODEL

The elementary units of granular materials, the “mesoscopic” particles, deform locally under stress at the contact point. The realistic modeling of this deformation would be computationally very expensive. Thus the interaction force is related to the overlap of two particles. As a further simplification, these two particles interact only if they are in contact (short range forces), and the force between them is decomposed into a normal and a tangential part.

The *normal force* is, in the simplest case, a linear spring that takes care of repulsion, and a linear dashpot that accounts for dissipation during contact.

$$f_i^n = k\delta + \gamma_0\dot{\delta}, \quad (1)$$

with spring constant k and some damping coefficient γ_0 . The half period of a vibration around the equilibrium position can be computed, and one obtains a typical contact duration (response time) $t_c = \pi/\omega$, with $\omega = \sqrt{(k/m_{ij}) - \eta_0^2}$, the eigenfrequency of the contact, the reduced mass $m_{ij} = m_i m_j / (m_i + m_j)$, and the rescaled damping coefficient $\eta_0 = \gamma_0 / (2m_{ij})$. The energy dissipation during a collision, as caused by the dashpot is quantified by the restitution coefficient $r = -v'_n / v_n = \exp(-\eta_0 t_c)$, where the prime denotes the normal velocity after a collision.

The *tangential force* involves dissipation due to Coulomb friction, but also some tangential elasticity that allows for stick-slip behavior on the contact level (Luding, 2004). In the static case, the tangential force is coupled to the normal force, Eq. (1), via Coulomb's law, i.e. $f^t \leq \mu_s f^n$, where for the limit sliding case one has the dynamic friction with $f^t = \mu_d f^n$. The dynamic and the static friction coefficients follow, in general, the relation $\mu_d \leq \mu_s$. However, for the following simulations, we will apply $\mu = \mu_d = \mu_s$. The static case requires an elastic spring in order to allow for a restoring force, i.e., a non-zero remaining tangential force in static equilibrium due to activated Coulomb friction.

If a contact exists with non-zero normal force, the tangential force can be active too, and we project the corresponding tangential spring into the actual tangential plane. This is necessary, since the frame of reference of the contact may have slightly rotated since the last time-step. $\vec{\xi} = \vec{\xi}' - \hat{n}(\hat{n} \cdot \vec{\xi}')$, where $\vec{\xi}'$ is the old spring from the last iteration, and \hat{n} is the normal unit vector. This action is relevant only for an already existing spring; if the spring is new, the tangential spring-length is zero, but its change is well defined for the next time-interval. The tangential velocity is $\vec{v}_t = \vec{v}_{ij} - \hat{n}(\hat{n} \cdot \vec{v}_{ij})$, with the total relative velocity of the contact surfaces of the particles (i,j):

$$\vec{v}_{ij} = \vec{v}_i - \vec{v}_j + a_i \hat{n} \times \vec{\omega}_i + a_j \hat{n} \times \vec{\omega}_j. \quad (2)$$

Next, we calculate the tangential test-force as the sum of the tangential spring and a tangential viscous force (in analogy to the normal viscous force):

$$\vec{f}_0^t = -k_t \vec{\xi} - \gamma_t \vec{v}_t, \quad (3)$$

with the tangential spring stiffness k_t and a tangential dissipation parameter γ_t . As long as $|\vec{f}_0^t| \leq f_c^s$, with

$f_c^s = \mu_s f^n$, one has *static friction* and, on the other hand, if $|\vec{f}_0^t| > f_c^s$, sliding, *dynamic friction* becomes active, with $f_c^d = \mu_d f^n$. Sliding is active as long as $|\vec{f}_0^t| > \mu_d f^n$, and is changed to sticking only as soon as $|\vec{f}_0^t| \leq f_c^d$ is reached. The corresponding states (static or dynamic) are kept in memory, to be used in the following time-step – and for contact statistics.

In the *static case*, the tangential spring is incremented, $\vec{\xi}' = \vec{\xi} + \vec{v}_t \Delta t_{MD}$, with the time step Δt_{MD} of the DEM simulation, to be used in the next iteration, and the tangential force, Eq. (3), is used.

In the latter, *sliding case*, the tangential spring is adjusted to a length, which is consistent with Coulombs condition

$$\vec{\xi}' = -(1/k_t)(f_c^d \hat{t} + \gamma_t \vec{v}_t), \quad (4)$$

with the tangential unit vector, $\hat{t} = \vec{f}_0^t / |\vec{f}_0^t|$, defined by the direction of the tangential test force above, and thus the magnitude of the sliding Coulomb force is used. Inserting the new spring length into Eq. (3) leads to $f_0^t \approx f_c^d$. Note that \vec{f}_0^t and \vec{v}_t are not necessarily parallel in three dimensions.

If all forces are known, acting on a selected particle (either from other particles, boundaries or external forces like gravity or a background damping $\vec{f}_i^b = -\gamma_b \vec{v}_i$), the problem is reduced to the integration of Newton's equations of motion for the translational and rotational degrees of freedom:

$$m_i \frac{d^2}{dt^2} \vec{r}_i = \vec{f}_i + m_i \vec{g} \quad \text{and} \quad I_i \frac{d}{dt} \vec{\omega}_i = \vec{\tau}_i, \quad (5)$$

with the gravitational acceleration \vec{g} , the mass m_i of the particle, its position \vec{r}_i , the total force $\vec{f}_i = \sum_c \vec{f}_i^c$, acting on it due to contacts with other particles or with the walls, its moment of inertia I_i , its angular velocity $\vec{\omega}_i$, and the total torque $\vec{\tau}_i = \sum_c \vec{l}_i^c \times \vec{f}_i^c$, with the center-contact ‘‘branch’’ vector \vec{l}_i^c .

In our DEM simulations, a three-dimensional tri-axial box is used. The walls are either fixed or stress controlled. Typical values of the test include a confining stress $p_0 = 1 \text{ kN/m}^2$, a wall-mass $m_w = 2 \text{ kg}$, and a viscosity of the wall, $\gamma_w = 200 \text{ kg/s}$, which corresponds to a viscous relaxation time $t_w = 0.01 \text{ s}$.

For the initial preparation of the sample, the spheres (with radii randomly drawn from a Gaussian distribution centered at 5 mm, a minimum of 3 mm and a standard deviation of 0.7 mm) were placed on a square lattice (big enough for them not to overlap). Then the box is compressed by imposing a confining pressure, p_0 , in order to achieve a homogeneous, isotropic initial condition. Inhomogeneities in the distribution of large and small particles were observed when the compression was performed too fast

and only from one side. The simulations presented below were compressed from all sides at the same time to avoid this effect. The preparation stage is finished when the kinetic energy becomes much smaller than the potential energy stored in the contacts. A periodic loading with period t_0 is applied next through a side of the box, while keeping the other stresses constant. The fact that all walls are stress controlled allows for a moving center of mass of the system. A more detailed study involving alternative boundary conditions is in progress.

3 RESULTS

Different friction coefficients and numbers of particles have been investigated: The systems studied have density $\rho=2000 \text{ kg/m}^3$, which leads to a mass $m=1 \text{ g}$ for a sphere with the mean radius $a=5 \text{ mm}$. The normal and tangential spring constants used (as described in the previous section) are $k_n=5000 \text{ N/m}$, and $k_t=1000 \text{ N/m}$, respectively. The following damping coefficient were applied: $\gamma_0=0.05 \text{ kg/s}$, $\gamma_t=0.01 \text{ kg/s}$, $\gamma_b=0.2 \text{ kg/s}$, $\gamma_{br}=0.05 \text{ kg/s}$, the latter two corresponding to background translational and rotational damping, respectively. This leads to a typical contact duration, $t_c=10^{-3} \text{ s}$, restitution coefficient, $r=0.95$, and background damping relaxation time, $t_b=0.005 \text{ s}$. The DEM step used is $\Delta t_{\text{MD}}=2.10^{-5} \text{ s}$, such that we can be sure that $\Delta t_{\text{MD}} < t_c < t_b < t_0$. If not explicitly mentioned, the friction coefficient is $\mu=0.1$. See Fig. 1 for a snapshot of a typical system.

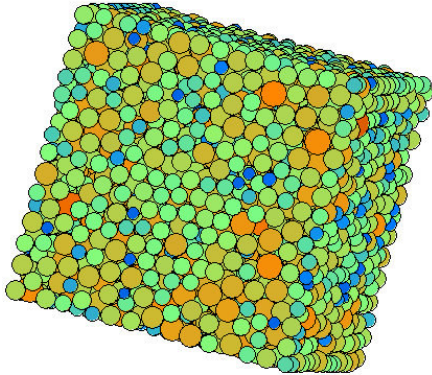


Figure 1: Snapshot of the model system with $N=3375$

3.1 System size

In order to examine effects of the system size on shakedown and ratcheting, and in order to learn whether it is possible to extrapolate this behavior to larger samples, four simulations with the same parameters were performed varying only the number of particles: $N=343, 1000, 1728$, and 3375 .

The stress is modified with the amplitude $\Delta\sigma=0.2p_0$, such that $2\sigma_{xx} := \sigma_{xx}^{\text{left}} + \sigma_{xx}^{\text{right}}$, and $2\sigma_{xx} = 2p_0 + \Delta\sigma[1 - \cos(2\pi t/t_0)]$, where t is the

time and $t_0=10 \text{ s}$ is the period of the cyclic loading. We performed also simulations with periods $t_0=20 \text{ s}$ and 40 s , and obtained no significant differences.

The deviatoric stress $\sigma_D = 2(\sigma_{xx} - \sigma_{yy})/3$ is plotted against the deviatoric strain $\epsilon_D = \epsilon_{xx} - \epsilon_{yy}$, in Fig. 2, with $\epsilon_{xx} = 1 - L_x/L_x^0$ and $\epsilon_{yy} = 1 - L_y/L_y^0$. The stress-strain relation consists of open hysteresis loops. The accumulated strain, ϵ_N , becomes smaller after each cycle until an approximately constant value is reached. The system size has a strong influence on strain accumulation, see Fig. 3. In the $N=343$ particle sample, the strain accumulation is constant after a few cycles. That means that the material adapts to the loading imposed, i.e., shakedown is reached.

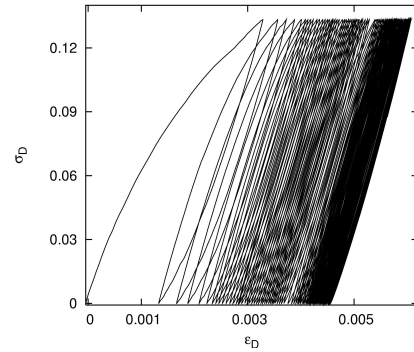


Figure 2: Deviatoric stress versus deviatoric strain in the first 100 cycles for a sample of $N=3375$ spheres

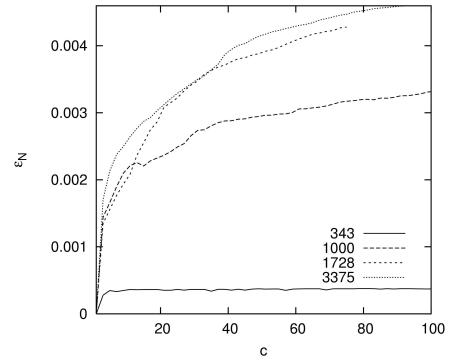


Figure 3: Strain accumulation, ϵ_N , as a function of the number of cycles, c , for different system sizes with N given in the inset

Larger systems show considerably stronger strain accumulation. Note that the largest two systems follow practically the same curve, showing ongoing strain accumulation even after 100 cycles, i.e., ratcheting is observed. From these results, we conclude that the shakedown limit lies well below a particle number of 1728, and that an extrapolation to larger systems is possible when samples of about 2000 particles are used – at least given the other parameters used here.

3.2 Effect of friction

We study the influence of friction, in a system containing $N=1728$ spheres, covering the friction coefficients, $\mu=0.1, 0.15, 0.20, 0.25$ and 0.5 . The effect of friction on the stress-strain relationship is clearly

observed already in the first cycle. In Fig. 4, the area enclosed by the cycle (which quantifies the dissipated energy in this cycle) is much smaller for stronger friction. This is also true after 100 cycles – data not shown here.

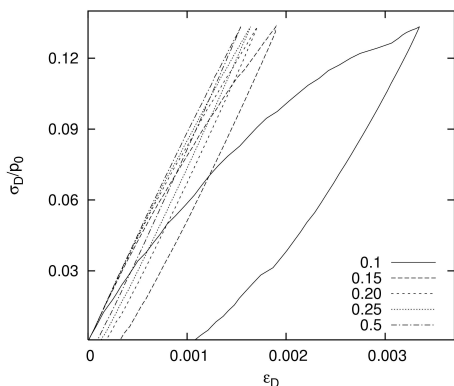


Figure 4: Deviatoric stress-strain relation for the first cycle for different coefficients of friction as given in the inset

The “elasto-plastic stiffness” of the material, given by the slope between the extreme points, increases as the friction increases and saturates for larger friction coefficients. This goes ahead with a decrease of the permanent strain accumulated in each cycle for higher friction. The system therefore crosses the boundary between ratcheting and shakedown when friction is decreased above $\mu=0.1-0.15$, see Fig. 5.

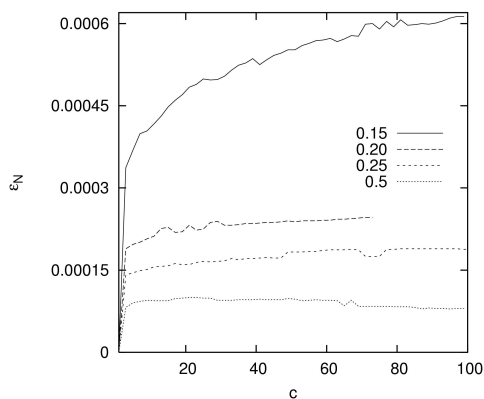


Figure 5: Strain accumulation, ϵ_N , as a function of c , for different coefficients of friction as given in the inset

4 DISCUSSION AND CONCLUSIONS

In summary, shakedown and ratcheting was examined in three dimensional model granulates consisting of polydisperse, frictional spheres. From our results we conclude that the limit between shakedown and ratcheting depends on both system size and friction: Very small systems show shakedown, while larger systems experience ratcheting, i.e., continuous increase of accumulated strain. Since increasing the system size above about 2000 particles leads to identical results, a system as small as possible is used to study the effect of friction. For the chosen magnitude

of deviatoric stress change, clear ratcheting is only observed for rather weak friction, while stronger friction seems to work against ratcheting by stabilizing the packing due to the stronger tangential forces.

The present study is only the first step towards a more detailed exploration of the influence of various other material- and system-parameters, involving variations of the stress amplitude, of the friction model, boundary conditions, and others.

ACKNOWLEDGEMENTS

The authors acknowledge support from the EU project Degradation and Instabilities of Geomaterials with Application to Hazard Mitigation (DIGA) in the framework of the Human Potential Program, Research Training Networks (HPRN-CT-2002-00220), the Deutsche Forschungsgemeinschaft (DFG), and FOM (Fundamenteel Onderzoek der Materie), financially supported by the Nederlandse Organisatie voor Wetenschappelijk Onderzoek (NWO).

REFERENCES

- Allen, M., P. Tildesley (1987). *Computer Simulation of Liquids*. Oxford: Oxford University Press.
- Alonso-Marroquin F. and H. J. Herrmann (2004). *Ratcheting of granular materials*, Phys. Rev. Lett. 92, 054301 (2004).
- Astumian, R. (2001). *Making molecules into motors*, Scientific American 58, 57-64.
- Colak, O. U. and E. Krempl (2003). *Modelling of uniaxial and biaxial ratcheting behavior of 1026 Carbon steel using the simplified Viscoplasticity Theory Based on Overstress*, Acta Mechanica (New York) 160, 27-44.
- García-Rojo, R. and H. J. Herrmann (2005). *Shakedown of unbound granular material*, Granular Matter 7(2), in press.
- Lekarp, F., U. Isacsson and Dawson A (2000). *Permanent strain response of unbound aggregates*, J. Transp. Engng.-ASCE 126 (1). 66-83.
- Luding, S. (2004), *Micro-macro transition for anisotropic, frictional granular packings*. Int. J. Sol. Struct. 41, 5821-5836.
- Luding S. (2004b), *Molecular dynamics simulations of granular materials*. In H. Hinrichsen and D. E. Wolf (Eds.), *The Physics of Granular Media*, Wiley VCH, Weinheim, Germany, pp 299-324.
- Vanel, L., D Howell, D. Clark, R.P. Behringer and E. Clement (1999), *Effects on construction history on the stress distribution under a sand pile*, Physical Review E 60, 5.